# Excited-State Forms of 2-Methylamino-6-methyl-4-nitropyridine *N*-Oxide and 2-Butylamino-6-methyl-4-nitropyridine *N*-Oxide

**Artur Makarewicz,[†] Anna Szemik-Hojniak,[‡] Gert van der Zwan,[§] and Irena Deperasińska*[,†]**

*Institute of Physics, Polish Academy of Sciences, Al. Lotników 32/46, 02-668 Warsaw, Poland, Faculty of Chemistry, University of Wroclaw, Joliot-Curie 14 st, 50-383 Wrocław, Poland, and Department of Analytical Chemistry and Applied Spectroscopy, Laser Centre, Vrije Universiteit, De Boelelaan 1083, 1081 HV Amsterdam, The Netherlands*

*Received: August 18, 2008; Revised Manuscript Received: February 12, 2009*

Excited-state quantum chemical calculations of two 2-alkyloamino-6-methyl-4-nitropyridine *N*-oxides are presented. Several different calculation methods and different basis sets were used, which all lead to similar results, although the precise values of excited-state energies and excited-state dipole moments differ. All methods used predict that in the $S_1$ excited state four types of isomers occur. In three cases, these excited-state local energy minima correspond to ground-state isomers, and these all have a $\pi\pi^*$ character. The fourth excited-state minimum, which we denote L*, does not have a corresponding ground-state isomer and has an $n\pi^*$ character. This isomer is stable and plays an important role in understanding the photophysics of these molecules. In addition, we also calculated barriers between these excited-state minima, using predescribed reaction pathways. The theoretical results derived in this Article are confronted with experimental data from earlier papers.

## 1. Introduction

The title compounds, 2-alkyloamino-6-methyl-4-nitropyridine *N*-oxides, have a complex structure: four functional groups with different electron−donor−acceptor properties attached to a $\pi$-electron aromatic system (see Figure 1). In addition, between two of these substituents, the pyridine NO and the aminoalkyl $-NHC_nH_{2n+1}$, an intramolecular N−H···O type hydrogen bond can occur.

The need to understand the properties of these molecules is common to many fields of molecular physics. They have been pointed out as good nonlinear optical materials,[1,2] they were found to be intermediates in organic chemistry,[3] and they are used to elucidate dissipation pathways of excitation energy in complex molecular systems.[4−7] These topics are not completely independent. For example, good candidates for nonlinear materials are molecules with low-lying charge-transfer states,[1,2,8,9] which often also play a role in relaxation mechanisms. The subject matter of this work concerns the last two of the above-mentioned topics. Two fundamental mechanisms that are investigated by molecular photophysics and photochemistry, excited-state charge transfer (CT) and excited-state proton transfer (PT), both occur in these *N*-oxides.[10−12] Moreover, it is worthwhile emphasizing that the investigated *N*-oxides are rare examples of nitro aromatic derivatives with measurable fluorescence. In general, these compounds are nonfluorescent.[12−16]

Our aim is to understand the processes these *N*-oxides undergo in the electronically excited state. This is needed for the interpretation of experimental data compiled so far,[4−7] that is, electronic absorption and steady-state and time-resolved emission spectra at a number of temperatures and in a variety of solvents. Measured under different conditions, these molecules exhibit a rather complex photophysical behavior and a nonexponential time decay. Below, we briefly review the experimental data available to us.

In this work, we theoretically examine the excited-state properties of the *N*-oxides, in particular the geometries in which they can appear. To that end, excited-state ab initio and TDDFT calculations were performed. Before looking at the experimental data, we make the following observations.

(i) 2M6M and 2B6M are closely related molecules (cf., Figure 1), but there are a few differences between them. For example, they have different crystal structures,[5,7] which is related to the way the molecules can form inter- and intramolecular hydrogen bonds. Extensive experimental data are available for both 2B6M and 2M6M. 2M6M, the smaller of these molecules, is the simplest object for calculations.

(ii) Experimental material is coming mainly from solutions, and solvent effects are taken into account using the Lippert and Mataga expressions.[17−19] Within the framework of this model, the energy of the molecule in the *k*th electronic state equilibrated to the solvent, $E_s(S_k)$, as compared to the energy of the molecule in the gas phase, $E_g(S_k)$, is given by:

$$E_s(S_k) = E_g(S_k) - \vec{\mu}^2(S_k) f_\varepsilon \quad (1)$$

with $k = 0, 1$ for the ground and first excited states, respectively. $E_g(S_k)$ is the energy of the molecule in the gas phase, and $\mu(S_k)$ is the dipole moment in the *k*th electronic state. The energy of the molecule in the so-called Franck−Condon (FC) state, resulting from a vertical electronic transition $l \rightarrow k$ (for absorption $l = 0$, $k = 1$ and for emission $l = 1$, $k = 0$), is given by the following expression:

$$E_s(S_k^{FC}) = E_g(S_k^{FC}) - \vec{\mu}^2(S_k^{FC}) f_n - \vec{\mu}(S_k^{FC})\vec{\mu}(S_l)(f_\varepsilon - f_n) \quad (2)$$

* Corresponding author. E-mail: deper@ifpan.edu.pl.
[†] Polish Academy of Sciences.
[‡] University of Wroclaw.
[§] Vrije Universiteit.

10.1021/jp8073927 CCC: $40.75 
Published on Web 03/20/2009

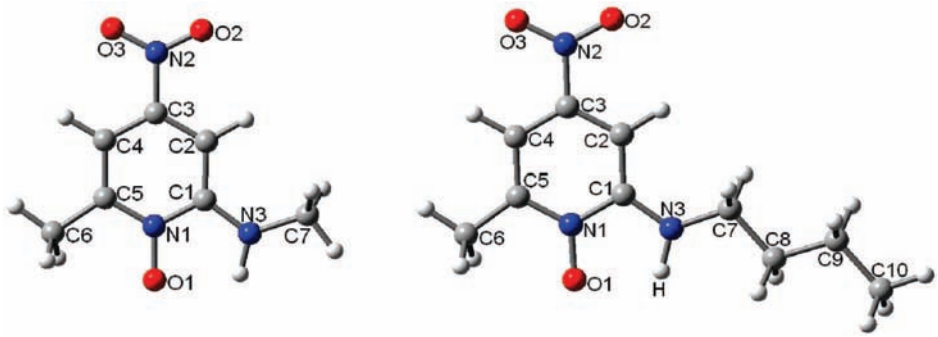


**Figure 1.** Molecular structures of 2M6M and 2B6M.

In these expressions, $f_\varepsilon$ and $f_n$ are solvent functions,[17] dependent on the dielectric constant $\varepsilon$ and the refractive index $n$ of solvent. In general, the values of $f_\varepsilon$ and $f_n$ increase with increasing $\varepsilon$ and $n$.[17] Therefore, the stabilization energy of equilibrated states increases with increasing dielectric constant of the solvent, and this increase is proportional to the square of dipole moment of molecule in the given state. The increase of stabilization energy of FC state is described by the inner product of the dipole moments characterizing the molecule in the initial and final FC state. All of our calculations were done for isolated (gas-phase) molecules, and corrections due to the expressions (1) and (2) applied afterward, for comparison to experimental results.

## 2. Summary of Experimental Data and Formulation of the Problem

In general, electronic excitation of the molecules studied in this Article leads to charge transfer between electron-donating and electron-accepting moieties, and as a consequence to changes in their properties in the excited state.[10] Conformational changes and excited-state proton transfer along the intramolecular hydrogen bond are examples of processes that can take place in the electronic excited state.[10−12] Such changes are reflected in fluorescence spectra by the observation of bands with anomalously large Stokes shifts or the appearance of new bands.[10−12]

In accordance with their complex structure, the *N*-oxides show complex photophysical and photochemical behavior.[4−7] The experimental results related to 2-methylamino-6-methyl-4 nitropyridine *N*-oxide (2M6M) and 2-butylamino-6-methyl-4 nitropyridine *N*-oxide (2B6M) (see Figure 1) can be summarized as follows:

(i) For both molecules, the transition energy corresponding to the first absorption band[5,7] is shifted to the red with increasing polarity of the solvent. Using eq 2, it is possible to estimate (by the least-squares method) that $\mu(S_1^{FC})\cdot\mu(S_0) \approx 38.65$ D$^2$ (for an Onsager sphere radius of 4.85 Å). The ground-state dipole moments $\mu(S_0)$ determined experimentally for similar *N*-oxides[20] are 3−4 D, and therefore $\mu(S_1^{FC})$ can be estimated as ∼9−10 D. This shows that the electronic excitation creates a state of large dipole moment or a CT state.

(ii) In the emission spectra, at least two fluorescence bands are observed, one of a normal (N) form and an anomalously Stokes shifted band (8000 cm$^{-1}$) (assigned to a tautomeric form in 4), denoted as T.

(iii) Apart from these two main bands, shoulders and weak peaks are observed, one of them coinciding with the emission maximum of solid 2B6M.[5]

(iv) Fluorescence of the N band is characterized by a short lifetime (of the order of 1−10 ps), whereas the T band has a much longer lifetime (100−150 ps).

(v) The intensity ratio between these two forms in the fluorescence spectra of both molecules is strongly solvent dependent: in weakly polar solvents, the N form dominates, whereas in a more strongly polar medium, the T form is predominant.[4−7]

(vi) Temperature decrease leads to a substantial increase of emission intensity in the T band as compared to the N band.[7]

(vii) In the case of 2B6M, it was found that the fluorescence quantum yield of the N band decreases significantly with increasing excitation energy.[6]

The presence of two fluorescence bands, characterized by distinctly different lifetimes, indicates the existence of at least two excited-state forms. On the basis of preliminary semiempirical and DFT calculations, mainly concerned with the ground state, the N band was assigned to the so-called normal form of alkyl amino *N*-oxides (Figure 1) and the T band to the excited-state tautomeric form with the proton transferred along the intramolecular N−H···O hydrogen bridge.[4] This transfer was experimentally estimated to be very fast, in acetonitrile within 100 fs.

These preliminary semiempirical ground-state calculations also showed that an $S_0 \rightarrow S_1$ excitation of the N form of 2-alkylamino-4-nitropyridine *N*-oxides gives rise to a substantial charge transfer in the molecule from the alkylamino group to the nitro group.[4,5,7,21] These results allowed us to tentatively explain the observed spectral shifts (i.e., changes of the transition energies between $S_0$ and $S_1$ states) with the increase of solvent polarity, but they cannot explain the above-described large change of the intensity ratio of the N and T bands. Such solvent effects resemble excited-state phenomena observed when polar entities are formed from the primary excited nonpolar molecular states, for example, TICT states.[10,12] However, according to the results of the semiempirical calculations, the dipole moments of both forms, N and T, were of comparable magnitude in the excited state.[5] Thus, the stabilization energies of both forms by the solvent should also be comparable. It is therefore of interest to check if the results of more advanced calculational methods give rise to similar conclusions.

The observed decrease of the fluorescence quantum yield in the N band upon increase of excess excitation energy also requires an explanation.[6] It was suggested that an additional path for excited-state proton transfer reaction is available in higher excited states.[6] Such a process is now deemed unlikely in the light of our knowledge of the properties of *N*-oxides in higher electronic states.[21]

Interest in the properties of excited states and paths of excited-state deactivation of nitro derivatives of aromatic compounds have given rise to extensive literature.[13−16,22−26] Enhancement of intersystem crossing and internal conversion by substitution with a nitro group are discussed in the literature, as well as the changes of the conformation of the nitro group in the excited state; these are thought to be of interest for the mutagenic

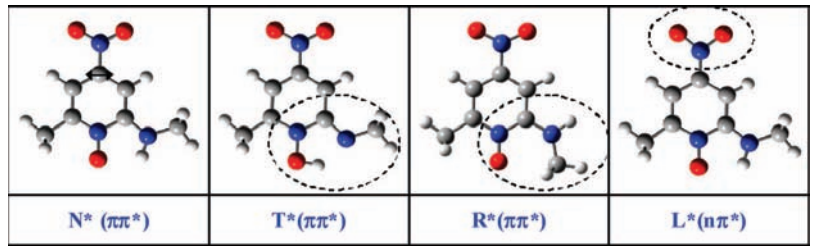


**Figure 2.** Schematic representation of stable forms of 2M6M in the electronic excited state.

potency of nitroaromatics.[27,28] The observations are also of interest for 2M6M and 2B6M.

All of the above problems strongly point to the need for theoretical investigation of excited-state potential energy surfaces for these *N*-oxides. The main goal of these calculations is identification of minima on the excited-state potential energy surface, determination of the properties of molecule in minimum energy geometries of the excited state, and discussion of experimental results in the light of the obtained calculation results. In the Calculation Methods section, we describe several methods, ab initio and DFT, used for the calculations.

The properties of the different isomers are discussed in the Calculation Results section. These include energies, dipole moments, and oscillator strengths of the transitions. We also identify geometries corresponding to a minimum in the excited-state potential surface, which do not have a corresponding minimal geometry in the ground state. In addition, we performed calculations of barriers for a number of possible reaction paths between the different geometries.

In the final section, Discussion and Conclusions, we then use these results to give a tentative explanation of the above list of experimental observations. It turns out that the structures found can indeed to a large extent explain observations given in earlier papers and form the basis of a kinetic model in nonpolar solvents. However, we finally have to conclude that still other excited-state isomers may be missing, for which we identify a possible candidate.

## 3. Calculation Methods

For the calculations, the Gaussian 03W[29] and Turbomole[30] programs were used. The latter program allows optimization of the geometry of molecules in the electronic excited states using the TDDFT (time-dependent density functional theory[31,32]) method and makes it possible to calculate relaxed excited-state dipole moments.[33]

The molecular geometries in the excited state were fully optimized, and for every optimized structure we verified that all of the vibrational frequencies were real and positive. The barriers separating different energy minima were calculated using the QST3 method of the Gaussian package.

It is well-known that the optimization and calculation of the energies of the molecular excited states has not yet achieved the accuracy of ground-state calculations. For example, the application of different calculational methods, such as TDDFT, CIS (configuration interaction with single excitations[34]), or CC2 (coupled cluster single and double excitations[35,36]), gives different transition energies of electronic transitions.[37−43] Therefore, precaution is needed for this kind of calculation. To exclude accidental results of one method, the optimization of excited states was performed using a number of different methods and different basis sets. We assume that when the same minimal energy geometries are given by all methods, they can be treated as highly probable.

The 2M6M molecule was optimized by TDDFT B3LYP/6-31G(d,p), CIS/6-31G(d,p), and CC2/cc-pVDZ methods in the excited state and by DFT B3LYP/6-31G(d,p), HF/6-31G(d,p), and CC2/cc-pVDZ methods in the ground state, while 2B6M molecule was optimized by TDDFT B3LYP/6-31G(d,p), CIS/6-31G(d,p), and CIS/6-31++G(d,p) methods in the excited state and by DFT B3LYP/6-31G(d,p), HF/6-31G(d,p), and HF/6-31++G(d,p) methods in the ground state. Because the CIS method is known to give transition energies higher than the corresponding experimental values,[34,35] spectroscopic properties of the structures optimized by the CIS method were calculated using the SAC-CI method of Nakatsuji and co-workers,[43] which is incorporated in Gaussian 03.

## 4. Results of the Calculations

Before presenting detailed results of the calculations, we want to point out that investigation of the electronically excited potential energy surface resulted in the determination of several local energy minima. Some of these are isomers similar to those in the ground state,[7] such as purely structural isomers, for example, the rotamers differentiated by rotation of the alkylamino group around the C1−N3 bond, but also tautomers formed by proton transfer along the intramolecular hydrogen bond. Yet besides those, structures were found that have no counterparts in the ground state. This lack of parallelism in different electronic states is determined by the different charge distributions of the molecules in these states and is known from other fields of molecular photophysics, examples being TICT states or excimers.[10−12]

Four excited-state structures (N*, T*, R*, and L*) of the 2M6M molecule in the $S_1$ state are found on the excited-state potential energy surface, which correspond to four minima of the potential energy, as shown in Figure 2 (excited-state optimization is indicated by the asterisk near the symbol of isomer). In three cases of the N*, T*, and R* forms, the $S_1$ state has $\pi\pi^*$ character, corresponding to a transition from the $\pi$-HOMO orbital localized on aminoalkyl group and aromatic ring to the $\pi^*$-LUMO orbital localized on the nitro group and the ring. However, in the case of the L* form, the $S_1$ state has $n\pi^*$ character and is described by transition from an n orbital localized on nitro group to a $\pi^*$-LUMO orbital localized as in previous cases on the nitro group and the ring. The shapes of all of these orbitals are shown in Figure 3.

**4.1. Geometries of the Excited-State Forms.** Detailed data on the 2M6M geometry (and of 2B6M for which analogous computations were performed) in the N*, T*, R*, and L* state are given in Table 1. Three of these structures, N*, T*, and R* (normal, tautomeric, and rotameric form), are in clear correspondence with the ground-state forms N, T, and R,[4,7] while the fourth one, L*, does not have an equivalent minimum in the ground state. It is characterized by a relatively small ONO angle of the nitro group. Similar small values of this angle have been found in the calculations of some of the excited states of

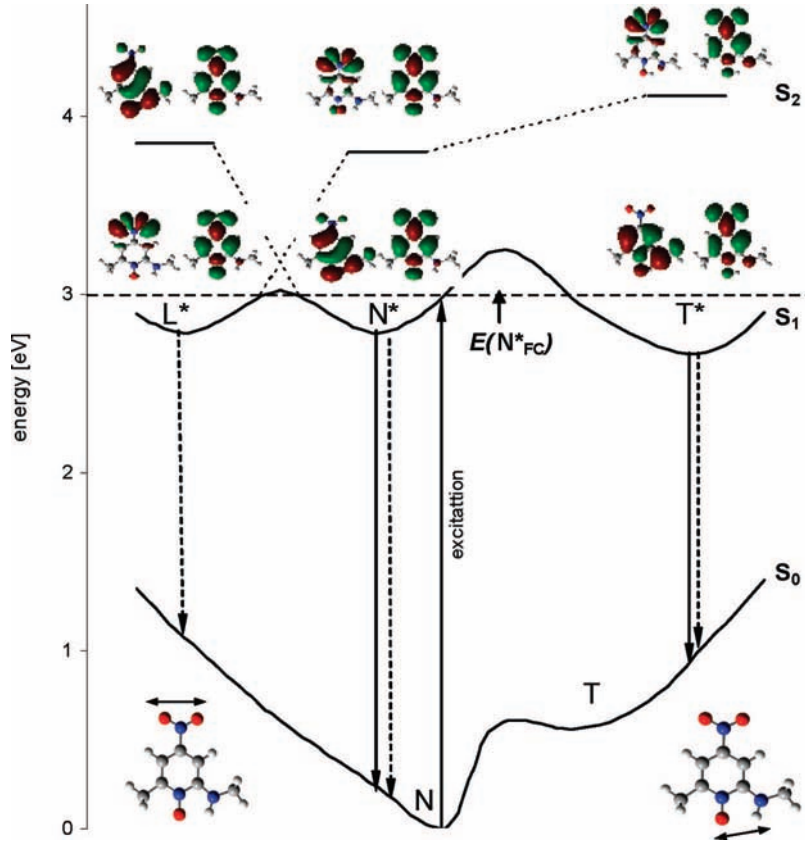


**Figure 3.** Energetic relationships between the isomers of 2M6M. The figure demonstrates the cross sections of the ground- ($S_0$) and excited-state ($S_1$) potential energy surfaces on the basis of calculation results by means of DFT and TDDFT B3LYP/6-31G(d,p) method. In the $S_0$ state, there are two minima; in the $S_1$ state, there are three energy minima (the L* isomer is stable only in the excited state). The reaction coordinate of the N* → T* transition is the proton position in the intramolecular hydrogen bond, while in the N* → L* reaction it is the ONO angle of the nitro group (symbolically represented in the lower corners of the figure). $E(N^*_{FC})$ is the energy level to which the excitation of the N form leads. Return to the ground state can be nonradiative (dashed arrows) or upon fluorescence emission (solid arrows). Above the energy minima (in the $S_1$ and in the $S_2$ state), the electronic configurations (pair of HOMO/LUMO orbitals) dominating in the description of the excited state of a given isomer are also displayed.

**TABLE 1: Geometric Parameters of the $S_1$ Excited-State Forms of 2M6M[a]**

| part of molecule | bond [Å] or angle [deg] | $S_0$ | $S_1$ | | | |
|---|---|---|---|---|---|---|
| | | N | N* | T* | R* | L* |
| NO | O(1)−N(1) | 1.292 | 1.308 | 1.369 | 1.306 | 1.297 |
| ring | N(1)−C(1) | 1.396 | 1.398 | 1.388 | 1.382 | 1.400 |
| | N(1)−C(5) | 1.373 | 1.363 | 1.359 | 1.378 | 1.379 |
| | C(1)−C(2) | 1.393 | 1.404 | 1.411 | 1.412 | 1.385 |
| | C(2)−C(3) | 1.390 | 1.387 | 1.390 | 1.381 | 1.414 |
| | C(3)−C(4) | 1.392 | 1.403 | 1.408 | 1.405 | 1.417 |
| | C(4)−C(5) | 1.387 | 1.397 | 1.388 | 1.389 | 1.378 |
| | N(2)−C(3) | 1.464 | 1.430 | 1.421 | 1.434 | 1.350 |
| $NO_2$ | O(2)−N(2) | 1.234 | 1.274 | 1.280 | 1.272 | 1.296 |
| | O(3)−N(2) | 1.232 | 1.277 | 1.276 | 1.274 | 1.296 |
| | ∠(O(2)N(2)O(3)) | 124.7 | 126.9 | 124.9 | 126.8 | 105.1 |
| $NH(CH_3)$ | N(3)−C(1) | 1.348 | 1.349 | 1.335 | 1.368 | 1.350 |
| intramolecular hydrogen bond | O(1)···H | 2.007 | 1.900 | 1.021 | | 2.017 |
| | O(1)···N(3) | 2.535 | 2.520 | 2.451 | 2.721 | 2.543 |
| | ∠(O(1)···HN(3)) | 109.6 | 115.6 | 129.0 | | 109.6 |
| | ∠(HN(3)C(1)) | 112.7 | 108.8 | 87.7112.9 | | |

[a] For comparison, also the ground-state structural parameters of the N-form[7] are presented. All results are obtained by means of the TD DFT B3LYP/6-31G(d,p) method. The numbering of atoms is shown in Figure 1.

the $NO_2$ molecule[44] and have been estimated from experiments on excited *p*-nitro-aniline.[9]

Comparison of excited-state geometries among each other and with the ground-state N form leads to the following conclusions:

(1) A common feature of all of the excited-state forms as compared to the ground-state geometry of 2M6M is an elongation of the N(2)O(2) and the N(2)O(3) bond lengths in the nitro group, and a shortening of the length of the bond with the ring (N(2)C(3)).

**TABLE 2: Energies and Dipole Moments of Ground- and Excited-State Structures of 2M6M Calculated by Means of Different Methods and with Different Basis Sets[a]**

| $S_1$ | TDDFT/6-31G(d,p) | | CIS/6-31G(d,p) | | CC2/cc-pVDZ | |
|---|---|---|---|---|---|---|
| structure | $E$ [eV] | $\mu$ [D] | $E$ [eV] | $\mu$ [D] | $E$ [eV] | $\mu$ [D] |
| N* | 0 | 9.49 | 0 | 6.65 | 0 | 10.58 |
| T* | −0.151 | 9.99 | −0.274 | 7.24 | −0.026 | 8.18 |
| R* | 0.268 | 9.91 | 0.331 | 9.27 | 0.018 | 10.90 |
| L* | −0.001 | 2.49 | −0.195 | 1.53 | −0.230 | 1.28 |
| $S_0$ | DFT/6-31G(d,p)[7] | | HF/6-31G(d,p) | | CC2/cc-pVDZ | |
| structure | $E$ [eV] | $\mu$ [D] | $E$ [eV] | $\mu$ [D] | $E$ [eV] | $\mu$ [D] |
| N | 0 | 3.35 | 0 | 2.14 | 0 | 3.44 |
| T | 0.562 | 2.98 | 0.334 | 3.04 | 0.530 | 2.54 |
| R | 0.411 | 2.83 | 0.376 | 1.90 | 0.279 | 2.49 |

[a] In each case, the energies of T*, R*, and L* forms are given with respect to the energy of N* form, and the energies of T and R with respect to the energy of N form. The heights of the barriers for N* to T*, L*, and R* transitions were calculated by the TD B3LYP/6-31G(d,p) method as 0.423, 0.289, and 0.905 eV and by the CIS/6-31G(d,p) method as 0.436, 0.197, and 0.375 eV.

**TABLE 3: Energies and Dipole Moments of Ground- and Excited-State Structures of 2B6M Calculated by Means of Different Methods and in Different Basis Sets[a]**

| $S_1$ | TDDFT/6-31G(d,p) | | CIS/6-31G(d,p | | CIS/6-31++G(d,p | |
|---|---|---|---|---|---|---|
| structure | $E$ [eV] | $\mu$ [D] | $E$ [eV] | $\mu$ [D] | $E$ [eV] | $\mu$ [D] |
| N* | 0.000 | 10.36 | 0.000 | 8.96 | 0.000 | 9.00 |
| T* | −0.135 | 10.23 | −0.263 | 9.05 | −0.217 | 9.49 |
| R* | 0.239 | 10.73 | 0.346 | 9.28 | 0.367 | 9.68 |
| L* | 0.032 | 2.96 | −0.172 | 2.01 | −0.067 | 2.10 |
| $S_0$ | DFT/6-31G(d,p) | | HF/6-31G(d,p | | HF/6-31++G(d,p | |
| structure | $E$ [eV] | $\mu$ [D] | $E$ [eV] | $\mu$ [D] | $E$ [eV] | $\mu$ [D] |
| N | 0.000 | 3.77 | 0.000 | 2.61 | 0.000 | 2.61 |
| T | 0.558 | 3.07 | 0.334 | 3.12 | 0.387 | 3.19 |
| R | 0.338 | 3.28 | 0.357 | 2.05 | 0.383 | 2.11 |

[a] In each case, the energies of the T*, R*, and L* forms are given with respect to the energy of the N* form and the energies of T and R with respect to the energy of the N form.

(2) The bond lengths of the aromatic ring of the L* form show that it has a quinoidal structure (and a small value of the (O(2)N(2)O(3) angle, as it was stated above).

(3) The most significant geometry differences between the N* and the T* forms are limited to those bonds that participate in intramolecular hydrogen bonding.

**4.2. Energies and Dipole Moments of the Excited-State Forms.** Data on the energies of different structures of both *N*-oxides, 2M6M and 2B6M, optimized in their electronic excited-state $S_1$ and in the ground $S_0$ state are collected in Tables 2 and 3.

The energetic relationships between ground and excited states of N*, T*, and L* forms are illustrated in Figure 3, which shows potential energy surfaces both in the ground and in the excited state. The curves shown here are the superposition of the two cross-sections: one along the reaction coordinate, which is taken as the proton position in the intramolecular hydrogen bond, and the second along the coordinate, which is taken as the ONO angle between the two NO bonds of the nitro group. In this last case, the passage along the reaction coordinate is connected with a change of electronic character of the $S_1$ state ($\pi\pi^* \leftrightarrow n\pi^*$). The transition N* ↔ L* can be considered a change in ordering of the excited states $S_1$ and $S_2$ in the molecule (see Figure 3) accompanied by changes of molecular geometry (see Table 1). The origin of nonzero interactions between them is a lack of symmetry in such complex structures. The mixing of $n\pi^*$ and $\pi\pi^*$ states, for example, was described in the case of excited states of nitrobenzene studied by CAS-SCF calculation by a $C_1$ symmetry.[23]

As one can see, there are three local energy minima (N*, T*, and L*) on the excited-state potential energy surface, while in the ground state there are only two, corresponding to the N and the T forms. The L* form does not have an equivalent minimum in the ground state. Comparing the energy of the N and T forms in both electronic states, it is obvious that in the ground state the N form has the lowest potential energy, $E(N) < E(T)$, whereas in the excited state this relation is inverted: $E(N^*) > E(T^*)$.

From the results presented in Tables 2 and 3 and Figure 3, we draw the following conclusions:

(i) All methods predict the excited-state isomers N*, T*, R*, and L* for both molecules.

(ii) All methods confirm the earlier conclusion[4,7] that in the ground state at ambient and lower temperatures only the N form is populated. Consequently, excitation of N to the Franck−Condon ($N^*_{FC}$) state initiates all excited-state processes.

(iii) The energy of the system in the excited FC ($N^*_{FC}$) state is near the top of the barrier for the $N^*_{FC} \rightarrow L^*$ transition (cf., Figure 3).

(iv) All methods give a higher energy of R* than that of the N*: $E(R^*) > E(N^*)$.

(v) However, the energetic relations between the N*, T*, and L* forms depend on the method: TD DFT predicts $E(N^*) \approx E(L^*) > E(T^*)$. CIS predicts $E(N^*) > E(L^*) > E(T^*)$. CC2 predicts $E(N^*) \approx E(T^*) > E(L^*)$.

Comparison of these results with the experiment is possible only for one case, for the difference $E(N^*) - E(T^*)$, which was estimated to be $\sim -0.18$ eV for 2M6M.[7] This value is close

**TABLE 4: Vertical Transition Energies and Oscillator Strength for the $S_1 \rightarrow S_0$ Transition and for $S_0 \rightarrow S_1(N^*_{FC})$ Transition in the 2M6M and 2B6M Molecules Calculated by Various Methods[a]**

| | 2M6M | | | | | | 2B6M | | |
|---|---|---|---|---|---|---|---|---|---|
| | TDDFT/6-31G(d,p) | | SAC CI//CIS/ 6-31G(d,p) | | CC2/cc-pVDZ | | TDDFT/6-31G(d,p) | | TDDFT/def-TZVP[4] |
| structure | $\Delta E$ [eV] | $f$ | $\Delta E$ [eV] | $f$ | $\Delta E$ [eV] | $f$ | $\Delta E$ [eV] | $f$ | $\Delta E$ [eV] |
| N* | 2.551 | 0.050 | 2.931 | 0.143 | 2.729 | 0.271 | 2.527 | 0.045 | 2.426 |
| T* | 1.723 | 0.019 | 2.202 | 0.079 | 1.897 | 0.031 | 1.715 | 0.025 | 1.937 |
| R* | 2.414 | 0.052 | 2.726 | 0.130 | 2.475 | 0.244 | 2.395 | 0.040 | |
| L* | 1.707 | 0.000 | 2.092 | 0.000 | 1.738 | 0.000 | 1.713 | 0.000 | |
| $N^*_{FC}$ | 2.998[7] | 0.074[7] | 3.335 | 0.137 | 3.358 | 0.211 | 2.973[5] | 0.071[5] | 2.897 |

[a] References 7 and 5 give the appropriate data of the $N^*_{FC}$ state, whereas ref 4 refers to the last column of 2B6M.

to the value −0.151 eV calculated by the TD DFT/6-31G(d,p) method (cf., Table 2).

(vi) The dipole moments of the N*, T*, and R* forms of both compounds are relatively large and of comparable magnitude. This conclusion is common to all methods used and confirms previously made estimates.[4,7]

(vii) The dipole moment of the excited N* form is larger by ∼6−7 D (depending on the method) as compared to the ground-state dipole moment. This value is in line with the difference of 6 D determined experimentally, based on solvent effects on the absorption spectra of 2B6M [see section 2 (i)].

(viii) The dipole moment of the L* structure is markedly smaller as compared to the dipole moments of the other forms in the excited state. Again, this conclusion is common for all calculation methods used.

(ix) The excited-state dipole moments of 2B6M are larger than those for 2M6M.

(x) Dipole moments obtained by the TDDFT method and by means of the CC2 method are slightly larger than those obtained by the CIS method.

**4.3. Energies of $S_1 \rightarrow S_0$ Electronic Transitions.** In Table 4, the spectral properties of the excited-state structures, that is, the vertical energies of the $S_1 \rightarrow S_0$ transitions and the corresponding oscillator strengths, are given. These data show that application of the TDDFT, SAC-CI, and CC2 methods leads to comparable results and also compares well with the experimental results. On the basis of the fluorescence spectra, the transition energies for the N* form are 2.76 and 2.74 eV for 2M6M and 2B6M, respectively, and for the T* form they are 2.13 and 2.08 eV. Therefore, we have a difference of ±0.2 eV as compared to the experimental results. Interestingly, the difference between the calculated energies of the $S_1 \rightarrow S_0$ transition from the N* and T* forms is ∼0.8 eV, similar to the experimental value.

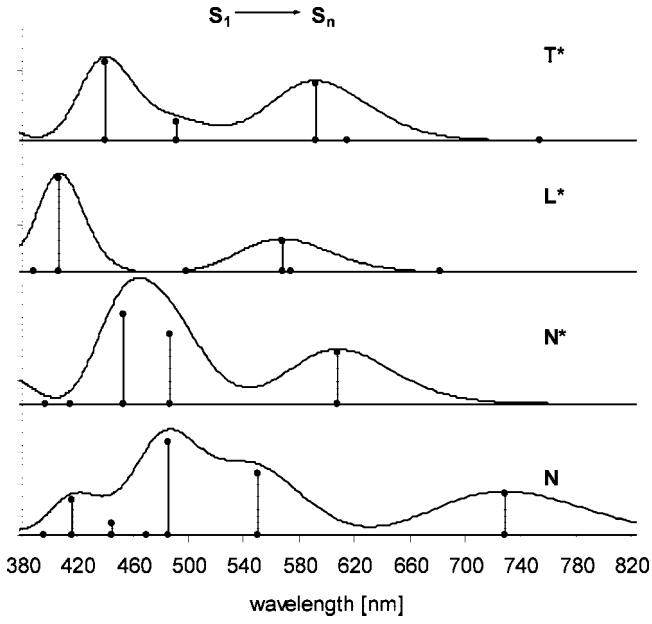


**Figure 4.** The $S_1 \rightarrow S_n$ spectra of N, N*, L*, and T* structures of the 2B6M molecule calculated by the TD DFT/6-31G(d,p) method. Each of the calculated lines is convoluted with a Gaussian distribution of a width comparable to the experimental bands.[4]

The results of calculations also show that the lowest excited state of the L* form is a dark state with practically zero oscillator strength ($f < 10^{-5}$). This is understandable because the n$\pi^*$ character of electronic configuration predominates in the description of L* (see Figure 3).

**4.4. Energies of $S_1 \rightarrow S_n$ Electronic Transitions.** Each of the structures optimized in the $S_1$ excited state may also be characterized by its transient absorption spectra, that is, by the $S_1 \rightarrow S_n$ transition energies, which should correspond to experimental transient absorption spectra. The results of the calculation are displayed in Figure 4. It is seen that each of the forms has a characteristic spectrum (although the absorption spectra are not much different for T*, L*, and N*, given the accuracy of calculations). In principle, this makes direct observation of the L* state possible. However, Figure 4 also reflects the scale of difficulties that one may encounter with the interpretation of transient absorption spectra. As can be seen, the spectra of particular forms are overlapping, and moreover in the course of time some of them will decrease in intensity, whereas others are growing in. From comparison with experimental spectra,[4] measured at an early stage of time evolution, a possible interpretation may be that the two bands (400 and 650 nm) observed immediately after excitation are related to absorption of two of the forms: vibrationally unrelaxed N* (according to the calculations a broadband at about 730 nm) and rapidly formed L* (calculated to be at 406 nm).

**4.5. Triplet State.** Figure 5 represents the system of singlet and triplet states of the N form of 2M6M. In the vicinity of the $S_1$ state, which is of $\pi\pi^*$ type, three triplet states $T_2$, $T_3$, and $T_4$ appear of $\pi\pi^*$-, $\pi\pi^*$-, and n$\pi^*$-type character, respectively. According to the El Sayed rules,[45] a strong spin−orbit coupling should involve only the pair of $S_1$, $T_4$ states, whereas the coupling of $S_1$ with $T_2$ and $T_3$ states should be much weaker. Such a state diagram resembles a situation characteristic of larger nitroaromatic hydrocarbons.[14]

## 5. Discussion and Conclusions

All of the different methods used show that in the $S_1$ state four basic isomeric forms are present. In three of the four forms, N*, T*, and R*, we are dealing with an excited state of $\pi\pi^*$

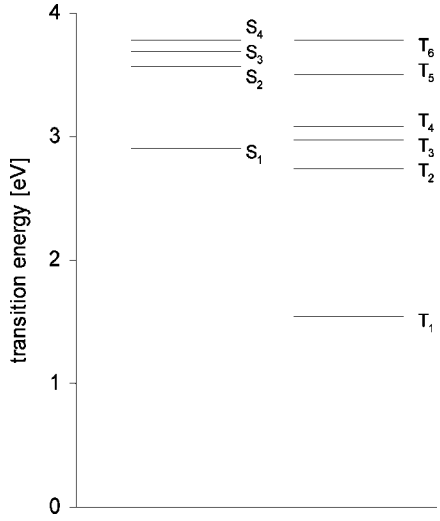


**Figure 5.** Singlet and triplet states of 2M6M (in N-form) calculated by the TD DFT/6-31G(d,p) method.

character with a large excited-state dipole moment, resulting from a partial charge transfer transition from the amino group and the ring to the nitro group. The orbitals of particular forms have different shapes, however, cf., the HOMO orbitals of the N* and T* forms in Figure 3.

The character of the lowest excited-state $S_1$ of the fourth form, L*, is different. It is an n$\pi$* state with a small excited-state dipole moment and with an almost zero oscillator strength for the transition to the ground state ($S_0$). This state may be compared to the nonfluorescent excited $S_1$ state of simple nitroaromatics. This points to the reason for the (uncommon) fluorescence of our *N*-oxides in the forms N*, R*, and T*. Substitution of the amino group creates a CT($\pi\pi$*) state with nonzero oscillator strength, which is now found to be below the n$\pi$* state. However, in the case of the L* form, the n$\pi$* state is still the lowest state, and in this form maintains the typical nonfluorescent properties of other nitro compounds.

**5.1. Calculations versus Experiment.** Calculational results of the excited-state geometry optimization of the two *N*-oxides are shown to reproduce such properties as their electronic spectra (i.e., the energies of $S_1 \rightarrow S_0$ electronic transitions for N* and T* forms; see section 4.3) and the dipole moment of the N* form (see section 4.2 (vii)). Also, the value of the energy gap $E$(N*) − $E$(T*), calculated by the TDDFT/6-31G(d,p) method, is close to the experimental result (see section 4.3 (v)). It is also possible to interpret the behavior observed in transient absorption spectra immediately after excitation as a trace of the presence of L* form (see section 4.4).

Therefore, the potential energy surfaces shown in Figure 3 are supported by experimental data. These are the absorption transition energy $N \rightarrow N^*_{FC}$, and emission energies from N* and T* to the respective ground states ($N^* \rightarrow N_{FC}$ and $T^* \rightarrow T_{FC}$, where $N_{FC}$ and $T_{FC}$ are ground-state FC states), that is, with the energy gap between the $S_1$ and $S_0$ surfaces at these three points. In addition, the energy difference between N* and T* in the $S_1$ state between is also reproduced. The calculations also confirm experimental results on the increase of the excited-state dipole moment for the N form, which was derived from the solvent polarity dependence.

**5.2. Photophysics of *N*-Oxides.** Figure 3 can also be used to illustrate the photophysics of the *N*-oxides. As we observed previously,[7] the $E$(T) − $E$(N) energy difference is so large that in the ground state at ambient and lower temperatures only the N form is populated, and hence its excitation to the Franck−Condon ($N^*_{FC}$) state initiates all excited-state processes.

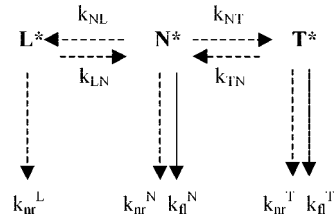


**Figure 6.** Scheme of excited-state processes of 2M6M and 2B6M compounds.

To these processes belongs vibrational relaxation in the excited state of the normal form $N^*_{FC} \rightarrow N^*$, when the molecule adapts its geometry to the desired charge distribution in the excited state. Besides that, we may be dealing with the transitions over or through the barriers that separate the N* structure from the minima of T* and L* (see Figure 3) as well as to the R* structure not shown in that figure. Returning to the ground state for all three forms may take place along a nonradiative path, but in the case of the N*, T*, and R* forms this can also happen by fluorescence emission as indicated by the results of the calculations shown above.

Hence, on the basis of calculations, we can propose a more complicated kinetic scheme of excited-state processes of the *N*-oxides than the one considered so far.[4−7] This new scheme is given in Figure 6.

In this, the possibility of a transition to the R* form and to the triplet states was omitted. All calculation methods show that the energy of the R* is higher than that of the N* form (see section 4.2 (iv)), and therefore the transition $N^* \rightarrow R^*$ is not effective. Similarly, in the light of the results described in section 4.5, the population of triplet states should be not effective (because of weak spin−orbit coupling between the $S_1$ state and all triplet states lying lower or at about equal energy with the $S_1$ state). However, in general, these processes cannot be completely excluded, and the scheme in Figure 6 can be considered somewhat simplified.

The solutions for the time dependence of the populations for this kinetics model are known.[46,47] These are, however, rather complicated expressions dependent on the nine rate constants, which should be viewed as parameters. Currently, we have insufficient experimental knowledge, and the solutions can give rise to many unexpected[48] but not necessarily real effects. Therefore, we only give a qualitative discussion of some of the results based on the above scheme.

On the basis of experiments in nonpolar solvents,[6] we now know the following: the quantum yields of emission for the N* and T* forms are $\Phi_f^N = 6 \times 10^{-4}$ and $\Phi_f^T = 1.5 \times 10^{-4}$, respectively, and the corresponding lifetimes of excited states are $\tau_N = 1.5 \times 10^{-11}$ and $\tau_T = 10^{-10}$ s. Applying the equations for the quantum yields, $\Phi_f^N = k_{fl}^N \tau_N$ and $\Phi_f^T = \Phi_{NT} k_{fl}^T \tau_T$,[39] one obtains that the quantum yield from population of the T* form is $\Phi_{NT} = 0.0375 k_{fl}^N / k_{fl}^T$. Taking the relation $k_{fl} \approx \nu^2 f / 1.5$[49] into account, where $f$ is the oscillator strength and $\nu$ is the transition energy in cm$^{-1}$, we find $\Phi_{NT} \approx 0.2$. Hence, the value of $k_{NT}$ (for $N^* \rightarrow T^*$ transition) may be estimated as $k_{NT} = \Phi_{NT}/\tau_N \approx 1.4 \times 10^{10}$ s$^{-1}$.

The value $\Phi_{NT} \approx 0.2$ means that other nonradiative processes compete with the $N^* \rightarrow T^*$ transition. The quantum yield of these other nonradiative processes can be estimated as $\Phi_{other} = 1 - \Phi_f^N - \Phi_{NT} \approx 0.8$. In general, these other processes can include $N^* \rightarrow N$ nonradiative transitions ($k_{nr}^N$), intersystem crossing to the triplet state, or the transition $N^* \rightarrow R^*$, which

were omitted in the scheme. According to our calculational results, the most important of these nonradiative ways may be the N* → L* process. According to the TD B3LYP/6-31G(d,p) calculations, the energy of the system in the excited FC state of the N form is near the top of the barrier for the $N^*_{FC}$ → L* transition (see Figure 2), which favors such transition.

The L* form does not fluoresce, and therefore there is no direct evidence of its existence. As stated above, a trace of L* could be found in the comparison of the calculation results for $S_1 \rightarrow S_n$ transitions with the early time transient absorption spectrum of 2B6M. Another indication of the presence of the L* form may be derived from the decrease of the quantum yield of the N* form upon excitation in the second absorption band.[6] This experimental result was originally explained by opening of an alternative channel through an excited-state proton transfer reaction.[6] However, according to the results of our earlier calculations,[5,21] excitation of the N form in the second absorption band is in fact an excitation to the fourth singlet state ($S_4$). The $S_0 \rightarrow S_4$ transition also has CT character, but now coming from charge transfer between the NO and $NO_2$ groups. At this excitation, the charge on the amino group does not change, and therefore the ability of amino group to facilitate proton transfer does not increase.

However, below the excited $S_4$ we now have an $S_2$ state that becomes the lowest state $S_1$ in the case of L* form (cf., Figure 3). In other words, the excitation of the normal form to $S_4$ is an excitation with an energy above the barrier for the N*→ L* transition. In that case, the relaxation of $S_4$ can lead not only to the $S_1$ state, but also to an N* → L* transition. If that is indeed the case, an increase of the quantum yield of the N* → L* transition (and a corresponding decrease of the population of N*) can be expected.

The most puzzling aspect, however, remains the observed polarity effect on the emission spectra of the *N*-oxides. In acetonitrile, practically only the T* form is visible. Its lifetime is only slightly longer ($\tau_T = 1.5 \times 10^{-10}$ s) than that in nonpolar solvents. This indicates that solvent polarity has no significant effect on the processes depopulating the T* form ($k_{fl}^T + k_{nr}^T$). If we assume that polarity of solvent does not change $k_{fl}^T$, the reason for the increase of emission intensity of T* relative to N* could be an increase of the $k_{NT}$ rate constant for the N* → T* process. This would be possible if the increase of polarity stabilizes the form T* with respect to the N* form. However, on the basis of our calculations, the dipole moments of both forms, N* and T*, are very similar. Therefore, it is not likely that medium polarity could significantly stabilize T* relative to N*.

It seems that the solution of this riddle must lie in the depopulation of the N* form. The increase of polarity of solvent causes shortening of its lifetime from $1.5 \times 10^{-11}$ to $5 \times 10^{-12}$ s. This indicates an increase of the rate constant for one of the nonradiative channels. However, because the dipole moment of L* is smaller than the dipole moment of N* (which means, in accordance with eq 1, that N* is stabilized relative to L* in polar solvents), an increase of $k_{NL}$ for the N*→ L* passage with increase of polarity of solvent is unlikely.

In all of these considerations, we have not yet introduced the height of barriers for particular transitions in the excited state. Although verification of barrier heights is difficult, one thing is clear from all calculations, a low barrier for the $N^*_{FC}$ → L* transition (and in case of femtosecond excitation due to the width of the excitation pulse, one may suppose that even a direct $N^*_{FC}$ → L* process may occur). Increase of polarity of the medium that leads to a stabilization of the N* relative to the L* state should inhibit the N*→ L* transition, resulting in population increase of the T* form. Indeed, experimentally, with increase of solvent polarity one can observe an intensity increase of the T*, but simultaneously a substantial shortening of the lifetime of the N* form is observed. It forces us to suppose that an explanation of the effect might be the appearance, in polar media, of an additional nonradiative channel depopulating N*, N* → X*. In some of our calculations, next to the above-mentioned N*, L*, R*, and T* structures, yet another form (X*) was found, although it was optimized only within one method [TD DFT B3LYP/6-31G(d,p)]. It is not meeting the criteria used in this work. According to those (see section 3), we have presented and disccussed only structures that were optimized within the framework of all methods employed. For this reason, X* is not presented in section 4 (results of the calculations). The X* form is displayed in Figure 7.

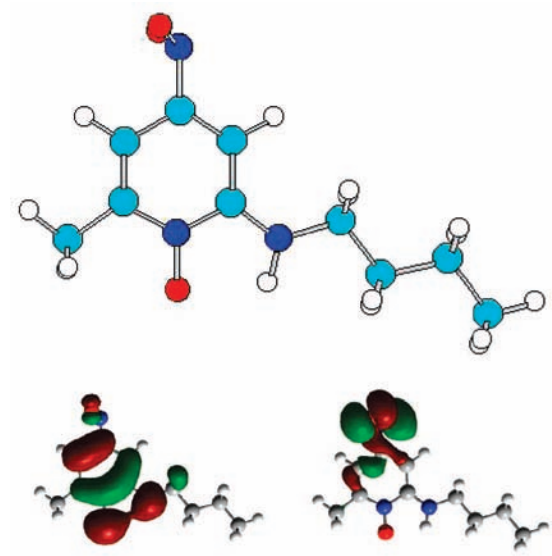

**Figure 7.** Structure of the X* form of 2B6 M and the shapes of the HOMO and LUMO orbitals in the $S_1$ state.

Similar to the L* form, it is a nonfluorescent structure with an energy significantly lower than that of N*, but with a large dipole moment of ∼13 D. Thus, it could be strongly stabilized in polar media and would be an ideal candidate to play the role of X*. It is characterized by a 90° rotation of the $NO_2$ group around its bond to the pyridine ring. Interestingly, this coordinate was assumed to be of relevance for relaxation mechanisms of excited nitrobenzene,[24] and it was also considered in the context of the biological activity of nitropolycyclic aromatics.[27,28] The reality of the X* structure will be the topic of further investigations.

**5.3. Concluding Remarks.** Within the framework of calculations presented in this work, a number of excited-state forms of 2-alkyloamino-6-methyl-4-nitropyridine *N*-oxides were identified. The calculated properties of these forms were discussed in the light of the existing experimental data, and it was demonstrated that they reproduce the observed electronic transition energies and dipole moments. The analysis of a kinetic scheme of excited-state processes in nonpolar solvents indicates that the most important pathway of decay of the primarily excited normal form N*($\pi\pi^*$) may be a transition to the L*(n$\pi^*$) form. The excitation process N + $h\nu$ → N* is of CT character, and the dipole moment of the N* form is large. In contrast, the dipole moment of L* is small. Therefore, the excitation of the N* form and transition to the L* form compose an interesting sequence of two fast CT processes. Further investigations of

these and related *N*-oxides with substituents at different positions can give insight into the possibilities of control of such a sequence of CT processes.

**Acknowledgment.** We thank the Interdisciplinary Centre for Mathematical and Computational Modelling in Warsaw for the use of its computational facilities (grant G32-10).

## References and Notes

(1) Gauillaume, M.; Botek, E.; Champagne, B.; Castet, F.; Ducasse, L. *J. Chem. Phys.* **2004**, *121*, 7390.
(2) Sosciun, H.; Castellano, O.; Bermudez, Y.; Toro-Mendoza, C.; Marcano, A.; Alvarado, Y. *J. Mol. Struct. (THEOCHEM)* **2002**, *592*, 19.
(3) Youssif, S. *Arkivoc* **2001**, 242.
(4) Poór, B.; Michniewicz, N.; Kállay, M.; Buma, W. J.; Kubinyi, M.; Szemik-Hojniak, A.; Deperasińska, I.; Puszko, A.; Zhang, H. *J. Phys. Chem. A* **2006**, *110*, 7086.
(5) Szemik-Hojniak, A.; Deperasińska, I.; Jerzykiewicz, L.; Sobota, P.; Hojniak, M.; Puszko, A.; Haraszkiewicz, N.; van der Zwan, G.; Jacques, P. *J. Phys. Chem. A* **2006**, *110*, 10690.
(6) de Klerk, J.; Szemik-Hojniak, A.; Ariese, F.; Gooijer, C. *J. Phys. Chem. A* **2007**, *111*, 5828.
(7) Wiśniewski, Ł.; Urbanowicz, A.; Jerzykiewicz, L.; Makarewicz, A.; Deperasińska, I.; van der Zwan, G.; Haraszkiewicz, N.; Puszko, A.; Szemik-Hojniak, A. *J. Mol. Struct.* **2009**, *920*, 45.
(8) Moran, A. M.; Kelley, A. M.; Tretiak, S. *Chem. Phys. Lett.* **2003**, *367*, 293.
(9) Moran, A. M.; Kelley, A. M. *J. Chem. Phys.* **2001**, *115*, 912.
(10) Grabowski, Z. R.; Rotkiewicz, K.; Rettig, W. *Chem. Rev.* **2003**, *103*, 3899.
(11) Tramer, A.; Jungen, Ch.; Lahmani, F. *Energy Dissipation in Molecular Systems*; Springer-Verlag: Berlin, 2005.
(12) Waluk J. In *Conformational Analysis of Molecules in Excited States*; Waluk, J., Ed.; Wiley-VCH: New York, 2000; pp 57−111.
(13) Morales-Cueto, R.; Esquivelzeta-Rabell, M.; Saucedo-Zugazagoitia, J.; Peon, J. *J. Phys. Chem. A* **2007**, *111*, 552.
(14) Mohammed, O. F.; Vauthey, E. *J. Phys. Chem. A* **2008**, *112*, 3823.
(15) Crespo-Hernandez, C. E.; Burdzinski, G.; Arce, R. *J. Phys. Chem. A* **2008**, *112*, 6313.
(16) Dobkowski, J.; Herbich, J.; Waluk, J.; Koput, J.; Kuhnle, W. *J. Lumin.* **1989**, *44*, 149.
(17) Beens, H.; Weller, A. In *Organic Molecular Photophysics*; Birks, J., Ed.; Wiley: London, 1976; p 159; solvent effect p 201.
(18) Deperasinska, I.; Dresner, J. *J. Mol. Struct. (THEOCHEM)* **1998**, *422*, 205.
(19) Parusel, A. B. J. *J. Photochem. Photobiol., B: Biol.* **2000**, *55*, 188.
(20) Pawełka, Z.; Lorenc, J.; Puszko, A. *J. Struct. Chem.* **2000**, *11*, 307.
(21) Deperasińska, I.; Makarewicz, A.; Szemik-Hojniak, S. *Acta Phys. Pol., A* **2007**, *112*, S-71.
(22) Sinha, H. K.; Yeates, K. *J. Chem. Phys.* **1990**, *93*, 7085.
(23) Takezaki, M.; Hirota, N.; Terazima, M.; Sato, H.; Nakajima, T.; Kato, S. *J. Phys. Chem. A* **1997**, *101*, 5190.
(24) Takezaki, M.; Hirota, N.; Terazima, M.; Sato, H. *J. Chem. Phys.* **1997**, *108*, 4685.
(25) Mondal, J.A.; Sarkar, M.; Samanta, A.; Ghosh, H. N.; Palit, D. K. *J. Phys. Chem. A* **2007**, *111*, 6122.
(26) Zugazagoitia, J. S.; Almora-Diaz, C. X.; Peon, J. *J. Phys. Chem. A* **2008**, *112*, 358.
(27) Li, Y. S.; Fu, P.P.; Chuch, J. S. *J. Mol. Struct.* **2000**, *550−551*, 217.
(28) Librando, V.; Alparone, A.; Zelica Minniti, Z. *J. Mol. Struct. (THEOCHEM)* **2008**, *856*, 105.
(29) Frisch, M. J.; Trucks, G. W.; Schlegel, H. B.; Scuseria, G. E.; Robb, M. A.; Cheeseman, J. R.; Montgomery, J. A., Jr.; Vreven, T.; Kudin, K. N.; Burant, J. C.; Millam, J. M.; Iyengar, S. S.; Tomasi, J.; Barone, V.; Mennucci, B.; Cossi, M.; Scalmani, G.; Rega, N.; Petersson, G. A.; Nakatsuji, H.; Hada, M.; Ehara, M.; Toyota, K.; Fukuda, R.; Hasegawa, J.; Ishida, M.; Nakajima, T.; Honda, Y.; Kitao, O.; Nakai, H.; Klene, M.; Li, X.; Knox, J. E.; Hratchian, H. P.; Cross, J. B.; Bakken, V.; Adamo, C.; Jaramillo, J.; Gomperts, R.; Stratmann, R. E.; Yazyev, O.; Austin, A. J.; Cammi, R.; Pomelli, C.; Ochterski, J. W.; Ayala, P. Y.; Morokuma, K.; Voth, G. A.; Salvador, P.; Dannenberg, J.; Zakrzewski, V. G.; Dapprich, S.; Daniels, A. D.; Strain, M. C.; Farkas, O.; Malick, D. K.; Rabuck, A. D.; Raghavachari, K.; Foresman, J. B.; Ortiz, J. V.; Cui, Q.; Baboul, A. G.; Clifford, S.; Cioslowski, J.; Stefanov, B. B.; Liu, G.; Liashenko, A.; Piskorz, P.; Komaromi, I.; Martin, R. L.; Fox, D. J.; Keith, T.; Al-Laham, M. A.; Peng, C. Y.; Nanayakkara, A.; Challacombe, M.; Gill, P. M. W.; Johnson, B.; Chen, W.; Wong, M. W.; Gonzalez, C.; Pople, J. A. *Gaussian 03*, revision D.01; Gaussian, Inc.: Wallingford, CT, 2004.
(30) Ahlrichs, R.; Bär, M.; Häser, M.; Horn, H.; Kölmel, C. *Chem. Phys. Lett.* **1989**, *162*, 165.
(31) Bauernschmitt, R.; Ahlrichs, R. *Chem. Phys. Lett.* **1996**, *256*, 454.
(32) Bauernschmitt, R.; Häser, M.; Treutler, O.; Ahlrichs, R. *Chem. Phys. Lett.* **1997**, *264*, 573.
(33) Amos, R. D. *Chem. Phys. Lett.* **2002**, *364*, 612.
(34) Foresman, J. B.; Head-Gordon, M.; Pople, J. A.; Frisch, M. *J. Phys. Chem.* **1992**, *96*, 135.
(35) Christiansen, O.; Koch, H.; Jørgensen, P. *Chem. Phys. Lett.* **1995**, *243*, 4041.
(36) Hättig, C.; Weigend, F. *J. Chem. Phys.* **2000**, *113*, 5154.
(37) Parac, M.; Grimme, S. *Chem. Phys.* **2003**, *292*, 11.
(38) Jamorski, Ch.; Foresman, J. B.; Thilgen, C.; Lütni, H.-P. *J. Chem. Phys.* **2002**, *116*, 8761.
(39) Nishimoto, K. *Internet Electron. J. Mol. Des.* **2002**, *1*, 572.
(40) Betowski, L. D.; Enlow, M.; Lee Riddick, L. *Comput. Chem.* **2002**, *26*, 371.
(41) Sancho-Garcia, J. C.; Perez-Jimenez, A. J. *J. Chem. Phys.* **2003**, *119*, 5121.
(42) Luke, V.; Aquino, A. J. A.; Lischka, H.; Kauffmann, H.-F. *J. Phys. Chem. B* **2007**, *111*, 7954.
(43) www.sbchem.kyoto-u.ac.jp/nakatsuji-lab.
(44) Grein, F. *Chem. Phys. Lett.* **2008**, *455*, 124.
(45) Turro, N. J. *Modern Molecular Photochemisty*; Benjamin/Cummings Publishing Co., Inc.: Menlo Park, CA, 1978; pp 103−117, 168, 176−184.
(46) Matsuzaki, A.; Nagakura, S.; Yoshihara, K. *Bull. Chem. Soc. Jpn.* **1974**, *47*, 1152.
(47) Rettig, W.; Majenz, W. *Chem. Phys. Lett.* **1989**, *154*, 335.
(48) Deperasińska, I.; Prochorow, J. *J. Mol. Struct.* **1997**, *436−437*, 585.
(49) Klessinger, M.; Michl, J. *Excited States and Photochemistry of Organic Molecules*; VCH Publishers, Inc.: New York, 1995; p 246.

JP8073927